Construction and Building Materials 200 (2019) 94–103

Contents lists available at ScienceDirect

Construction and Building Materials

journal homepage: www.elsevier.com/locate/conbuildmat

Effect of freeze-thaw cycles on the mechanical behavior of geopolymer concrete and Portland cement concrete containing micro-encapsulated phase change materials

Shima Pilehvar [a,b], Anna M. Szczotok [a,c], Juan Francisco Rodríguez [c], Luca Valentini [d], Marcos Lanzón [e], Ramón Pamies [b], Anna-Lena Kjøniksen [a,*]

[a] Faculty of Engineering, Østfold University College, P.O. Box 700, 1757 Halden, Norway
[b] Department of Materials Engineering and Manufacturing, Technical University of Cartagena, Cartagena, Murcia, Spain
[c] Department of Chemical Engineering, University of Castilla – La Mancha, 13004 Ciudad Real, Spain
[d] Department of Geosciences, University of Padua, 35131 Padua, Italy
[e] Departamento de Arquitectura y Tecnología de la Edificación, Escuela Técnica Superior de Arquitectura e Ingeniería de Edificación ETSAE, Universidad Politécnica de Cartagena, 30203 Alfonso XIII 52, Cartagena, Spain

HIGHLIGHTS

- Addition of micro-encapsulated phase change materials to concrete reduce the adverse effect of freeze-thaw cycles.
- Geopolymer concrete maintains the compressive strength better after freeze-thaw cycles than Portland cement concrete.
- The setting times of geopolymer paste becomes much faster when the temperature is decreased from 20 to 0 °C.
- Microcracks is observed in the concrete structure after the freeze-thaw cycles.

ARTICLE INFO

Article history:
Received 6 August 2018
Received in revised form 2 December 2018
Accepted 12 December 2018
Available online 22 December 2018

Keywords:
Geopolymer concrete
Portland cement concrete
Micro-encapsulated phase change materials
Freeze-thaw cycles
Compressive strength
Setting times
Microstructure

ABSTRACT

The effect of frost conditions on the physical and mechanical properties of geopolymer concrete (GPC) and Portland cement concrete (PCC) containing two different micro-encapsulated phase change materials (MPCM) was examined. Microstructural studies revealed that the freeze-thaw induced concrete deterioration can be contributed to microcracks appearing at the weak interfacial transition zones between paste/aggregate and paste/MPCM. The addition of MPCM provided an excellent resistance against freeze-thaw cycles with minor reduction of the compressive strength, unlike the samples without MPCM where a stronger reduction was observed. When the temperature was reduced to 0 °C, the initial setting time of Portland cement pastes became longer due to the low temperature and the high viscosity. For geopolymer pastes, the initial setting time became shorter due to phase separation of the alkaline solution at low temperatures. Increasing the MPCM concentration reduced the final setting time for both Portland cement and geopolymer pastes.

1. Introduction

Recycling waste materials into new building materials helps conserve the environment and natural resources. Geopolymers are an interesting alternative to ordinary Portland cement, and noticeably diminish greenhouse gas emission and reduces the high energy consumption compared to Portland cement [1–3]. Geopolymers can be prepared from industrial waste materials that are rich in aluminosilicate or kaolinite combined with an alkaline solution [4,5]. In addition, geopolymer compositions exhibit excellent mechanical performance and shorter setting times in comparison to cementitious materials [6–8].

In cold climates such as the Scandinavian countries, buildings are exposed to freezing weather during winter. This is one of the main causes of mortar and concrete degradation [9,10]. Phase change materials (PCM) can result in the structure being exposed to fewer freeze-thaw cycles, and can help maintaining a comfortable indoor temperature [11,12]. When the temperature is higher than the melting point of PCM, extra heat is absorbed by

* Corresponding author.
E-mail address: anna.l.kjoniksen@hiof.no (A.-L. Kjøniksen).

https://doi.org/10.1016/j.conbuildmat.2018.12.057
0950-0618/

the melting of the PCM, which has a high latent heat. When the temperature decreases, the PCM releases the excess heat by solidification [13,14]. Encapsulating the PCM into microcapsules prevents interactions between the PCM and the surrounding materials. In addition, microcapsules provide a large heat transfer surface area, and increase the structural stability [15,16]. Better thermal comfort can be achieved by using mortar and concrete containing micro-encapsulated phase change materials (MPCM). However, the MPCM has a negative effect on the mechanical properties of construction materials [17–22].

The effect of freeze-thaw cycles on the mechanical properties of cementitious and geopolymer compositions have been examined previously [23–27]. However, as far as we know the effect of MPCM addition on the freeze-thaw induced changes of compressive strength, mass loss and microstructure of geopolymer concrete and Portland cement concrete have not been previously reported.

The objective of this study is to investigate how MPCM integration affects the mechanical properties of both geopolymer concrete (GPC) and Portland cement concrete (PCC) after exposure to freeze-thaw cycles. In addition, the effect of MPCM at frost conditions on the early-age properties of GPC and PCC has been investigated.

2. Materials and methods

2.1. Materials

Two different MPCMs with hydrophobic shells (to minimize the amount of water adsorbed onto the shell of the microcapsules) were utilized. PE-EVA-PCM, has a shell that is a copolymer of 50 wt% low density polyethylene (LDPE) and 50 wt% ethylvinylacetate (EVA) [28]. St-DVB-PCM, has a shell consisting of a copolymer of 50 wt% styrene (St) and 50 wt% divinylbenzene (DVB) [29]. A paraffin wax (Rubitherm®RT27) is used as the core of both microcapsules. Fig. 1 shows SEM images the utilized microcapsules. It should be noted that PE-EVA-PCM exhibits a non-spherical geometry and contains high amounts of agglomerates while St-DVB-PCM have a spherical shape [18,22].

In order to prepare geopolymer concrete, an alkaline activator solution, class F fly ash (FA), ground granulated blast furnace slag (GGBFS), sand, and gravel were used. Sodium hydroxide pellets and sodium silicate solution (35 wt% solid) used for preparing the alkaline solution were purchased from VWR, Norway.

The FA and GGBFS were provided from Norcem and Cemex, Germany, respectively. Table 1 shows chemical compositions determined by X-ray fluorescence (XRF) of GGBFS and class F fly ash.

Table 1
Analysis of FA and GGBFS by X-ray fluorescence.

Constituents	FA (wt%)	GGBFS (wt%)
Al_2O_3	23.15	10.3
SiO_2	50.83	34.51
CaO	6.87	42.84
Fe_2O_3	6.82	0.6
MgO	1.7	7.41
K_2O	2.14	0.52
TiO_2	1.01	0.66
Na_2O	1.29	0.39
P_2O_5	1.14	0.02
SO_3	1.24	1.95
SrO	0.19	0.05
CO_2	3.07	0.3

In order to obtain a better workability without adding high amounts of water, a superplasticizer (FLUBE OS 39 from Bozzetto Group, Italy) was utilized.

Portland cement II mixed with FA (Blaine fineness of 4500 cm^2/g), was obtained from Norcem, Norway. A superplasticizer (Dynamon SR-N from MAPEI, Norway) was utilized to gain a better workability without adding more water.

The gravel and sand (Gunnar Holth and Skolt Pukkverk AS) utilized for both geopolymer concrete and Portland cement concrete originated from Råde and Mysen, Norway, respectively. The size distributions of the components displayed in Fig. 2 was determined by mechanical sieving (EN 933-1) for gravel and sand, and by low angle laser light scattering (Malvern Mastersizer 2000) for MPCM, GGBFS, and FA.

2.2. Mixing, casting and curing methods

For all geopolymer mixtures, an alkaline solution with a ratio between the sodium silicate solution and the sodium hydroxide solution (14 M) of 1.5 and a total SiO_2 to Na_2O ratio of 0.7 was selected. The details of the alkaline solution preparation is explained in Pilehvar et al. [30]. Since the paste does not contain sand, the microcapsules were added as an extra additive. For the concrete mixtures, the microcapsules replaced a corresponding volume of sand [22].

For geopolymer paste, an alkaline solution to geopolymer binder (Fly ash + GGBFS) ratio of 0.4 was selected to reach the standard consistency described in EN 196-3. The geopolymer binder and alkaline solution were mixed together for 90 s; after which the microcapsules were added and mixed for 90 s to achieve a

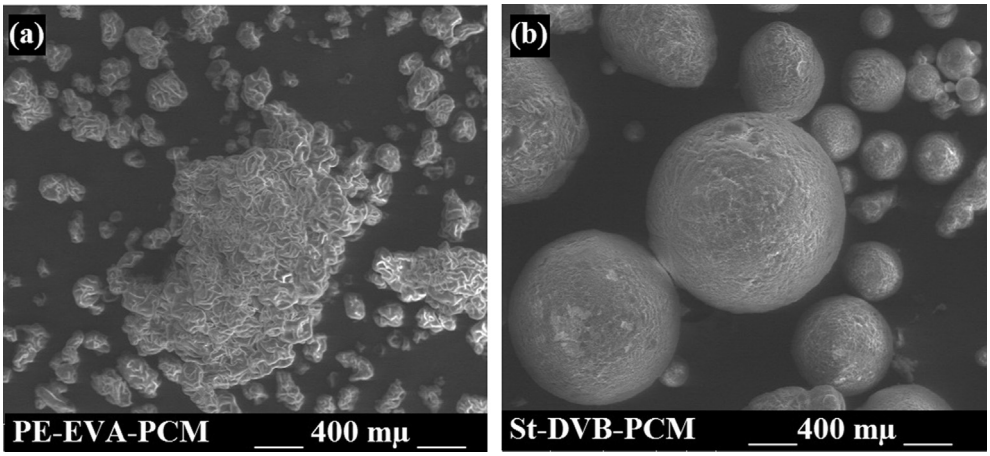

Fig. 1. Morphology of the microcapsules captured by SEM (a) PE-EVA-PCM (b) St-DVB-PCM.

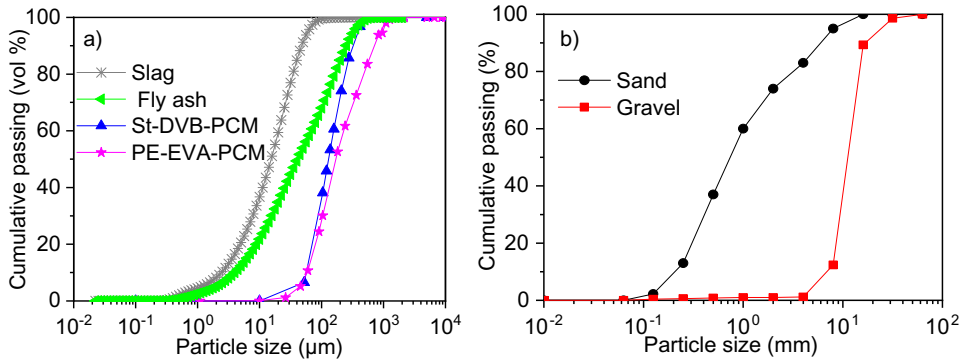

Fig. 2. Particle size distributions of (a) slag, fly ash, and microcapsules, and (b) sand and gravel.

homogenous paste. For Portland cement paste, water and cement with a water to cement ratio of 0.35 was mixed for 90 s to achieve the same consistency as the geopolymer paste. After adding MPCM, the mixing was continued for an additional 90 s. For both geopolymer and Portland cement pastes, the MPCM was added as an additional 20 vol% of powder materials.

In order to have comparable data for GPC and PCC, the total amount of liquid (alkaline solution + extra water) to the geopolymer binder and the water to cement ratio for the Portland cement were kept constant at 0.5. In addition, the combined amount of gravel and sand for the concretes without microcapsules was nearly the same for geopolymer concrete and Portland cement concrete. The details of GPC and PCC preparations are described previously [22,30].

To reduce potential damage to the microcapsules due to the mixing process, they were the last component added to the mixtures [31]. The compositions of geopolymer and Portland cement pastes and concretes are given in Table 2 and Table 3, respectively. For concrete, the percentages of microcapsules correspond to the volume of sand replaced by MPCM.

The GPC and PCC samples where 0 and 20% of the sand was replaced by St-DVB-PCM or PE-EVA-PCM, were cast as described in Pilehvar et al. [22] at 20 °C. Due to the short setting time of GPC, a vibration machine was used to remove air trapped inside the specimens whereas for the PCC samples, a steel pestle was used to compact the molds. After casting GPC and PCC into 10 × 10 × 10 cm molds, they were pre-cured for 24 h (ambient temperature; relative humidity of 90%), after which the samples were demolded. The demolded samples were cured in tap water for 28 days at 20 °C. Before starting the freeze-thaw cycles, the cured samples were kept in open air for 1 h (to help remove surface water) and weighed. For each freeze-thaw cycle, the samples were first immersed in tap water located in a cooling room at a temperature of 3 ± 1 °C for 6 h. Afterward, the samples were left in a freezer at a temperature of −20 ± 1 °C for 18 h. The samples were subjected to 0, 7, 14, and 28 freeze-thaw cycles. After the freeze thaw cycles, the samples were gently dried at room temperature before further testing.

Table 2
Mix design of geopolymer paste and concrete. The concrete recipe gives 1 m^3 of mixture.

Materials	Paste (kg)		Concrete (kg)	
	MPCM 0%	MPCM 20%	MPCM 0%	MPCM 20%
Alkaline solution	188.5	188.5	189.8	189.8
Fly ash	280.2	280.2	280.2	280.2
GGBFS	191	191	191	191
Sand	–	–	828.1	662.5
Gravel	–	–	809.6	809.6
Extra water	–	–	47	47
Superplasticizer	–	–	4.8	4.8
MPCMs	0	35	0	55.8

Table 3
Mixture design of Portland paste and concrete. The concrete recipe gives 1 m^3 of mixture.

Materials	Paste (kg)		Concrete (kg)	
	MPCM 0%	MPCM 20%	MPCM 0%	MPCM 20%
Cement	471.2	471.2	471.2	471.2
Water	165	165	235.6	235.6
Sand	–	–	957	765.6
Gravel	–	–	705	705
Superplasticizer	–	–	4.8	4.8
MPCMs	0	28.3	0	64.3

2.3. Testing methods

The mineralogical characterization study of GPC and PCC containing 0 and 20% of the microcapsules after 0 and 28 freeze-thaw cycles, was carried out using a Hitachi S3500N scanning electron microscope (SEM) utilizing an accelerating voltage of 15 kV. A back-scattered electrons (BSE) detector was applied for imaging. Unpolished samples were coated with platinum in a sputter coater Polaron SC7640 before measurements.

The internal microstructure of PCC and GPC containing 0 and 20% microcapsules after 0 and 28 freeze-thaw cycles was examined by X-ray tomographic scans, utilizing a Skyscan 1172 CT scanner (Bruker) with 85 kV incident radiation, 800 ms exposure time per frame and a rotation step of 0.3°. The final sets of vertically stacked slices (voxel size of 6 μm) were reconstructed using the Feldkam algorithm [32]. The measurements were performed on cylindrical specimens (1 cm diameter and 1 cm height) drilled from the samples utilizing a Skyscan 1172 (Bruker, Billerica, US).

The percentage of mass loss was calculated to examine the influence of freeze-thaw cycles on the concrete degradation and MPCM loss:

$$\textit{Percentage mass loss} = \frac{\theta_0 - \theta_{cycle}}{\theta_0} \times 100$$

where θ_0 and θ_{cycle} are the mass of the sample before and after the freeze-thaw cycles, respectively. In addition to the standard freeze-thaw cycles, GPC and PCC containing 0% and 20% microcapsules, were stored outdoors for three months (November to January, Fredrikstad, Norway) to examine the effect of exposure to real weather conditions. After outdoor exposure, the mass loss was mea-

sured in the same way as for the freeze-thaw cycles. The reported values are the average of the three cubes.

The compressive strength tests after 0, 7, 14, and 28 freeze-thaw cycles were performed at 20 °C in accordance with EN 12390-3, using a digital compressive strength test machine (Form + Test Machine) with a force at a loading rate of 0.8 kN/s. Before the measurements, three cubes were left at ambient conditions for 1 h (to help remove surface water and ice), after which they were weighed and measured. Additionally, the compressive strength of GPC and PCC containing 0% and 20% microcapsules, after three months outdoor exposure was measured. The reported values are the average of the three cubes.

The setting times of Portland cement and geopolymer pastes without microcapsules and with 20% microcapsules were carried out at 0 °C and 20 °C with a computer controlled Vicat needle instrument (ToniSET One, Model 7301). To conduct the measurements at 0 °C, the instrument basin was filled with an ice/water mixture. The setting time was calculated from the initial mixing of the raw materials, and measured with an interval of 10 min for Portland cement paste and 2 min for geopolymer paste. The initial setting time is the time when the needle penetration is less than 39.5 mm whereas the final setting time is the moment when the needle penetrates the sample to a depth of 0.5 mm.

3. Results and discussion

3.1. Freeze-thaw cycles

3.1.1. Microstructural study

Microscopical structure chracterization of GPC and PCC containing St-DVB-PCM and PE-EVA-PCM after 0 and 28 freeze-thaw cycles were performed by SEM and X-ray tomography imaging. SEM images of the samples after 28 freeze-thaw cycles are shown in Fig. 3. In Fig. 4, the samples containing microcapsules are displayed at a higher maginfication. The transition zone between the MPCM and the concrete matrix depends on the microcapsule shell [22], and hydrophobic materials usually exhibit poor adhesion to a cementitious matrix [33]. This causes visible gaps between the microcapsules and the concrete matrix for both PCC and GPC (Fig. 3b, c, e, f, Fig. 4), illustrating that the bonds between the concrete and MPCM are poor. This might affect the concrete mass loss and the strength reduction after repeated freeze-thaw cycles.

From Fig. 3a it is evident that crystals are formed in PCC as one of the hydration products during the freeze-thaw cycles (similar crystals are not observed before the freeze thaw cycles). Fig. 4a and c shows that in the presence of microcapsules, crystalls form in the gap between the microcapsules and the concrete matirx. Crystal formation is expected to reduce the compressive strength of PCC by expansion and an increase of solid volume [34,35].

For GPC, microcracks are formed after the freeze thaw cycles (Fig. 3d). In addition, microcrackes are present after the freeze thaw cycles of all samples (both GPC and PCC) containing PCM (see Fig. 3b, c, e, f). Microcracks are not visible in the SEM-image of PCC without microcapsules (Fig. 3a). This might be due to the extensive crystal formation (Fig. 3a), which might hide microcracks formed underneath the crystalls. Formation of microcracks is expected to contribute to the concrete deterioration.

2D X-ray micro-tomography cross-sectional slices of GPC and PCC without MPCMs are shown in Fig. 5. In these images, bright colors are associated with components with high X-ray attenuation such as sand and gravel, whereas components with low or no X-ray attenuation (air voids and MPCM) are displayed in dark colors. The field of view is approximately 1 cm. Fig. 5A, a, D and d show the microstructural changes of PCC and GPC without MPCMs before and after exposure to freeze-thaw cycles. After the freeze-thaw cycles, microcracks are evident in the PCC matrix (Fig. 5a) and at the interfacial transition zone between geopolymer paste and the

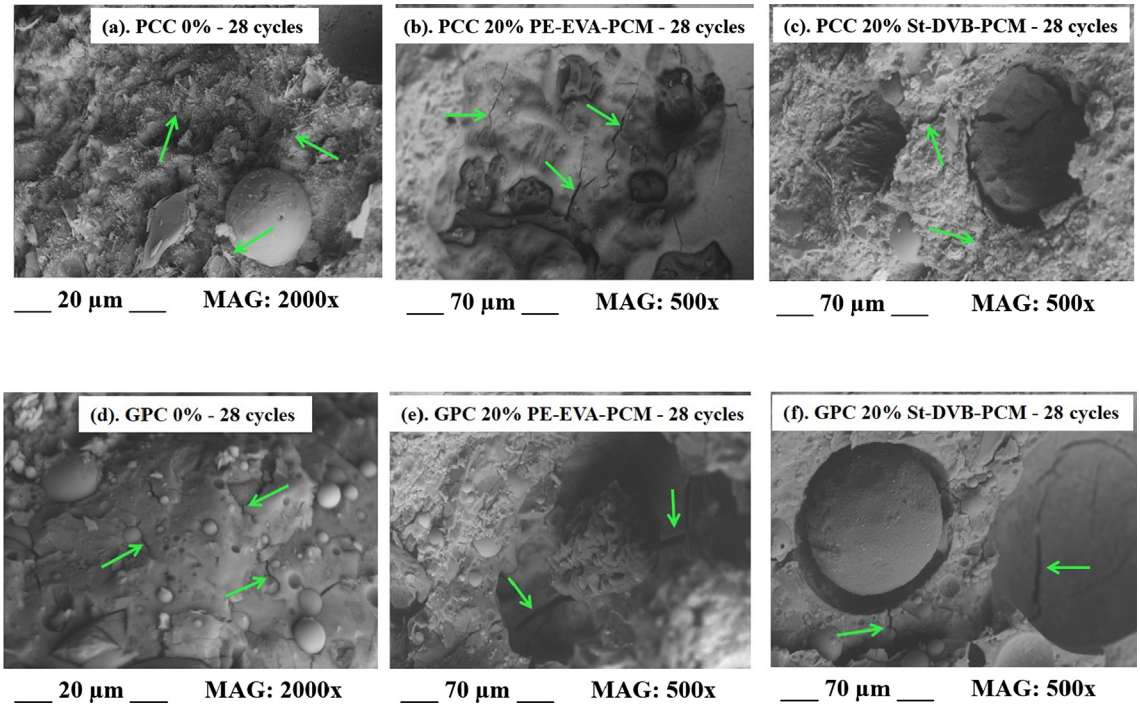

Fig. 3. SEM images of the fracture surface of (a) PCC 0% – 28 cycles (the arrows show crystal formation) the rounded particle is fly ash, (b) PCC 20% PE-EVA-PCM – 28 cycles (the arrows show microcracks in the matrix), (c) PCC 20% St-DVB-PCM – 28 cycles (the arrows show microcracks in the matrix), (d) GPC 0% – 28 cycles (the arrows show microcracks in the matrix), (e) GPC 20% PE-EVA-PCM (the arrows show microcracks in the matrix), and (f) GPC 20% St-DVB-PCM after 28 freeze-thaw cycles (the arrows show microcracks in the matrix).

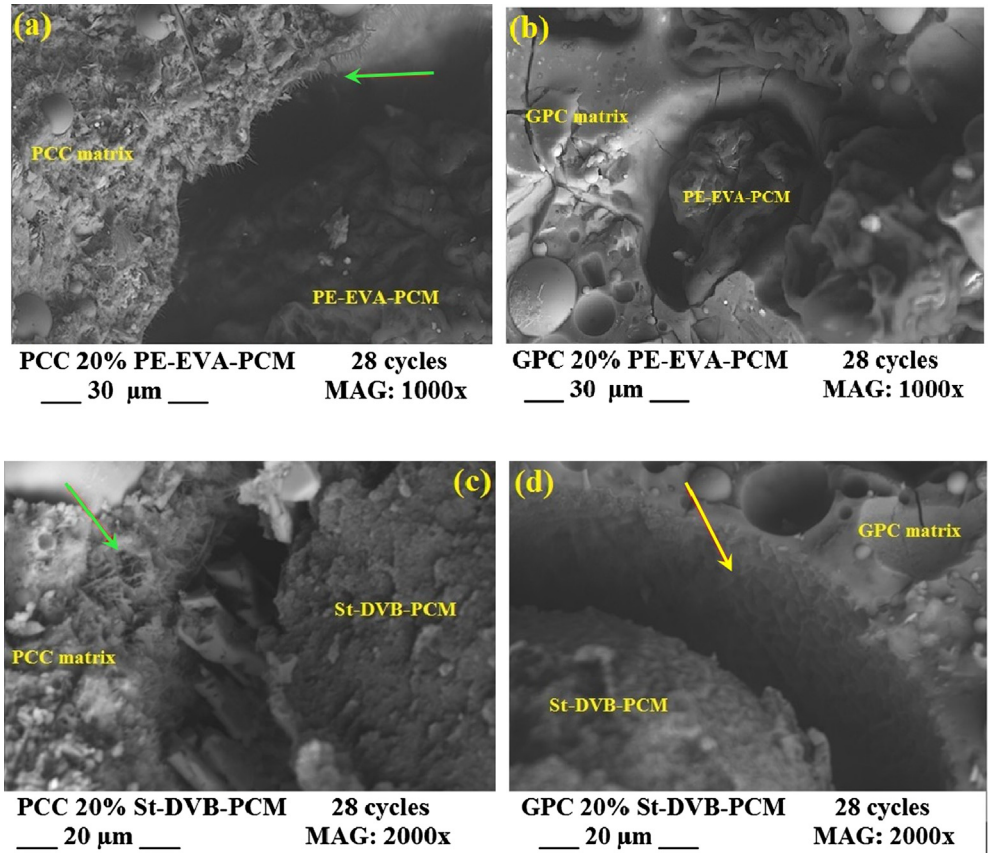

Fig. 4. SEM images of (a) the PCC matrix and PE-EVA-PCM, the arrow shows crystalized structures located in the gap between matrix and MPCM. (b) The GPC matrix and PE-EVA-PCM, the weak interfacial transition zone is visible. (c) The PCC matrix and St-DVB-PCM, the arrow shows crystalized products located in the gap between matrix and MPCM. (d) The GPC matrix and St-DVB-PCM, the arrow shows the trace of microcapsule shell on the gap between the microcapsules and the concrete matrix.

gravel (Fig. 5d, e, f). This indicates that the generated microcracks provoked by freeze-thaw cycles are contributing to the damage and deterioration of PCC and GPC. Interestingly, microcracks are not observed between the PCC paste and the aggregates in the presence of the MPCM after the freeze-thaw cycles (Fig. 5b, c). This illustrates that stronger bonds are formed between the PCC paste and the aggregates than for GPC where microcracks are evident (Fig. 5d, e, f). As can be seen from the images, the inclusion of MPCM's led to a substantial increase of porosity, thus reducing the mechanical performance of the materials.

3.1.2. Mass loss

Freeze-thaw cycles can erode the concrete. It is, therefore, interesting to examine the mass loss for GPC and PCC with and without MPCM. Fig. 6 illustrates that when the percentage of MPCM increases, the mass loss after 28 cycles becomes higher for both GPC and PCC. This might be due to the soft nature of the microcapsules and their poor connection to the concrete matrix (as is evident from the gaps between the concrete and MPCM in Fig. 3). This can cause the MPCM to be easily eroded from the surface. In addition, MPCM can weaken the concrete structure, which might render it less resistant to freeze-thaw erosion. Despite the MPCM erosion and visible microcracks on the surfaces of samples, there is not any sign of concrete spalling. For PCC without MPCM, the mass loss is negative (i.e., the samples gain weight). This is probably due to water being adsorbed within pores and microcracks [36,37]. The weight gain of PCC without MPCM during the freeze thaw cycles illustrates that determination of mass loss is not a suitable method for concrete durability evaluation. Earlier studies also found that the mass loss is not an accurate measure of the concrete degradation [38].

To evaluate the effect of real weather conditions, GPC and PCC with and without microcapsules were left outdoors from the 16th of October 2017 until the 16th of January 2018 in Fredrikstad, Norway. The mass loss of PCC are less than for the samples exposed to freeze-thaw cycles (Fig. 7a, Fig. 6a). This is probably due to less severe outdoor conditions compared to the freeze-thaw test. As can be seen from Fig. 7b, the temperature fluctuations during this time period were moderate compared to the freeze thaw cycles. Interestingly, the PCC samples gain weight (negative weight loss). This might be due to adsorption of water in microcracks [36,37]. As can be seen in the insets of Fig. 8a, the samples were submerged in snow for parts of the period.

3.1.3. Compressive strength

Fig. 8 shows the compressive strength and the compressive strength reduction of PCC and GPC with incorporated microcapsules after 0, 7, 14, and 28 freeze-thaw cycles. As observed previously, GPC exhibits better compressive strength than PCC and incorporation of MPCM cause a decrease of the compressive strength [22]. The freeze-thaw induced changes in compressive strength of GPC is less than 5% at all conditions, showing that the strength of GPC from this recipe is stable against freeze thaw cycles both with and without added microcapsules. However, PCC without MPCM exhibit a pronounced strength reduction as a result of the freeze thaw cycles. The most important reason for the deterioration is expansion of water in the permeable concrete when it freezes. The volume of water increases by about 9% when it freezes [39], which generates a hydraulic pressure within the sample. Air voids within the sample provides space the ice can expand into. However, when the available free space is filled up the freezing ice exerts a pressure on the surrounding concrete matrix. When

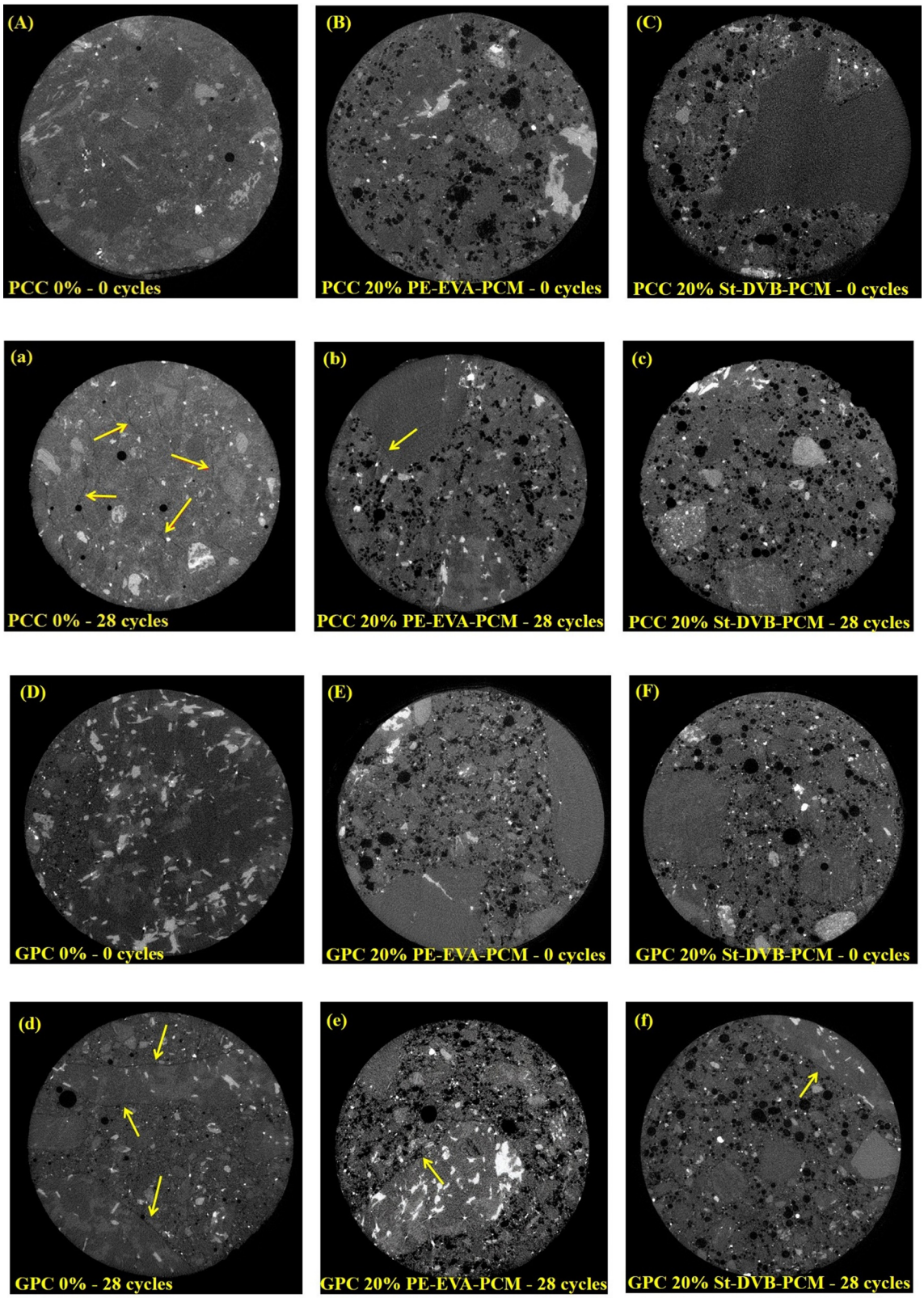

Fig. 5. 2D X-ray-tomography images of samples (A) PCC 0% – 0 cycles, (a) PCC 0% – 28 cycles, (B) PCC 20% PE-EVA-PCM – 0 cycles, (b) PCC 20% PE-EVA-PCM – 28 cycles, (C) PCC 20% St-DVB-PCM – 0 cycles (c) PCC 20% St-DVB-PCM – 28 cycles, (D) GPC 0% – 0 cycles, (d) GPC 0% – 28 cycles, (E) GPC 20% PE-EVA-PCM – 0 cycles, (e) GPC 20% PE-EVA-PCM, (F) GPC 20% St-DVB-PCM – 0 cycles, and (f) GPC 20% St-DVB-PCM after 28 freeze-thaw cycles. The arrows show the gap in interfacial transition zone and microcracks in the concrete matrix.

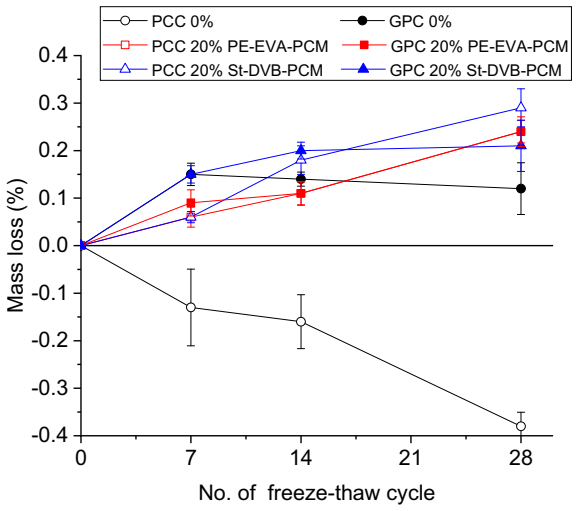

Fig. 6. Variation of mass loss with the number of free-thaw cycles.

the force overcomes the tensile stress of concrete, microcracks are created and cause concrete degradation (Fig. 3) [25,40,41]. This is expected to reduce the compressive strength [25,41–43]. Since the initial compressive strength of GPC is higher than for PCC, it can withstand higher pressures from the freezing water before microcracks are formed. In the absence of microcapsules, the strength reduction of GPC is therefore less than for PCC.

Interestingly, the compressive strength of the samples containing MPCM are not significantly affected by the freeze-thaw cycles. MPCM addition increases the concrete porosity by causing more air voids to form in the concrete matrix [20,44]. In addition, the air gaps between MPCM and the concrete matrix (Fig. 3, Fig. 4) provide available space within the concrete structure [22,45]. These air voids can improve the frost resistance of concrete by acting as expansion reservoirs for the freezing water and thereby reduce frost induced stress [46].

As for the freeze thaw cycles, there is little effect on the compressive strength of GPC after three months exposure to outdoor conditions (Fig. 9a). Interestingly, for PCC the compressive strength after three months exposure to outdoor conditions is actually higher than before exposure to the environment (Fig. 9b). Since the outdoor conditions are less severe than the freeze-thaw cycles (Fig. 7b), the degradation of the concrete strength is probably moderate. The increased compressive strength suggest that the hydration reaction is continuing during the time the samples are stored outside, thereby contributing to an increased compressive strength [47–49].

3.2. Setting times

Fig. 10 shows the effect of temperature and microcapsules on the setting times of Portland cement and geopolymer pastes. It is clear from Fig. 10 that the geopolymer reaction is much faster than the hydration of Portland cement (note the differences in the scaling of the y-axis). As expected, decreasing temperature slows down the hydration of Portland cement paste [50], resulting in longer setting times. Interestingly, the setting times for geopolymer pastes are much faster at low temperatures.

When MPCM is added to cement paste, water is adsorbed on the surface of the microcapsules, thereby reducing the amount of available water in the paste [30,51]. Although a reduction of available water is expected to speed up the cement hydration during the initial stage of the hydration process [52–54], the initial setting time becomes longer when microcapsules are added to the samples. This is probably caused by a higher viscosity, which can slow down the initial stage of the cement reaction [30, 55–57]. PE-EVA-PCM exhibits a more pronounced effect on the initial setting time since it adsorbs much more water and has lower slump (higher viscosity) than St-DVB-PCM [30]. After the initial setting time, the viscosities are high for all samples. At this stage, the faster cement hydration due to the reduced amount of available water becomes the dominant process. Accordingly, the solidification of the samples is faster and the final setting time becomes shorter for the samples containing microcapsules [30].

For geopolymer paste at ambient temperature, a similar behavior has been observed previously [30]. However, at 0 °C, the setting times are very fast without a significant effect of microcapsule addition. The solubility of NaOH in water decreases from 1110 g/L (27.8 M) at 20 °C to 418 g/L (10.5 M) at 0 °C. In addition, the solubility of sodium silicate also becomes lower when the temperature is reduced. The exact values depend on the sodium silicate composition, and the solubilities will probably also be affected

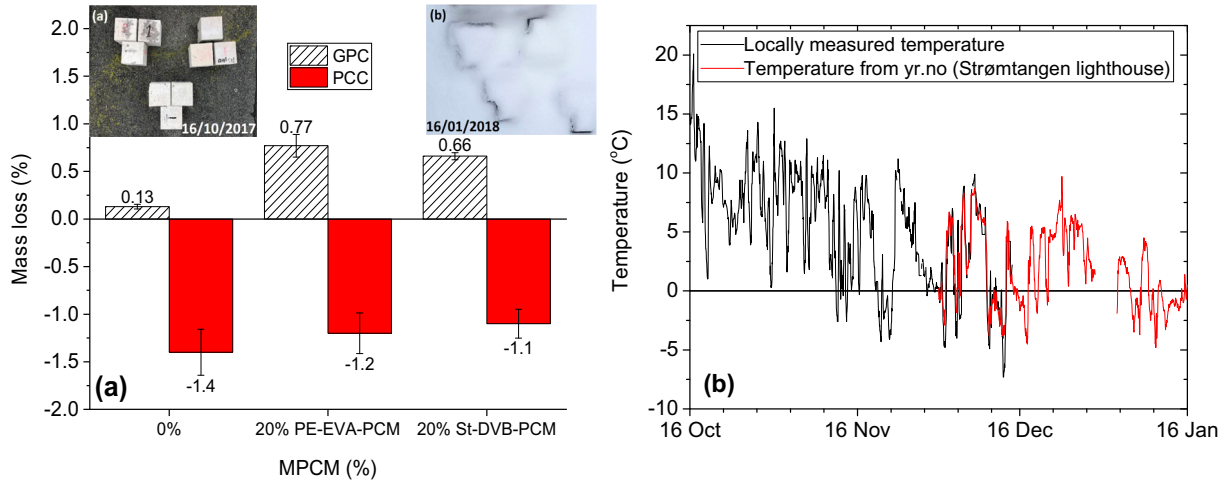

Fig. 7. (a) Mass loss for PCC and GPC with and without MPCM after three months at outdoor conditions. The inset pictures illustrate the outdoor conditions which varies between a non-frozen environment in October (left inset) to sub-zero temperatures and snow in January (right inset), (b) temperature fluctuations during these three months. The weather station located next to the samples broke down during the measurements, which is why the temperature during the last month is represented by data from yr.no at Strømtangen lighthouse about 9 km SW of the measuring site. The 2 week overlap between the two measuring sites show that they are in reasonably good agreement with each other.

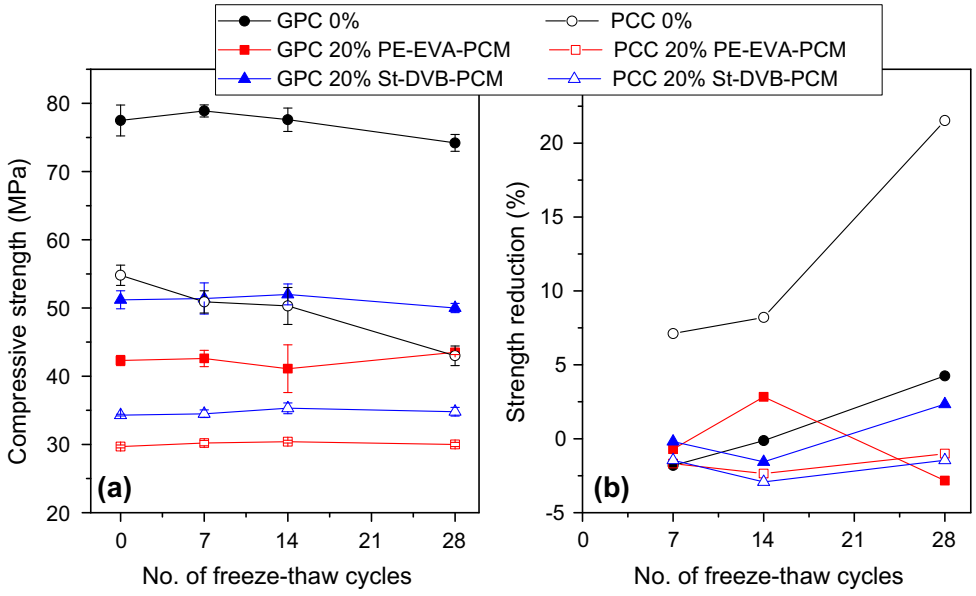

Fig. 8. (a) Compressive strength of GPC and PCC versus the number of freeze-thaw cycles when 0 and 20% sand is replaced by microcapsules, (b) the compressive strength reduction (percentage of initial compressive strength of the corresponding samples without microcapsules at the same curing time) for PCC and GPC versus the number of freeze-thaw cycles.

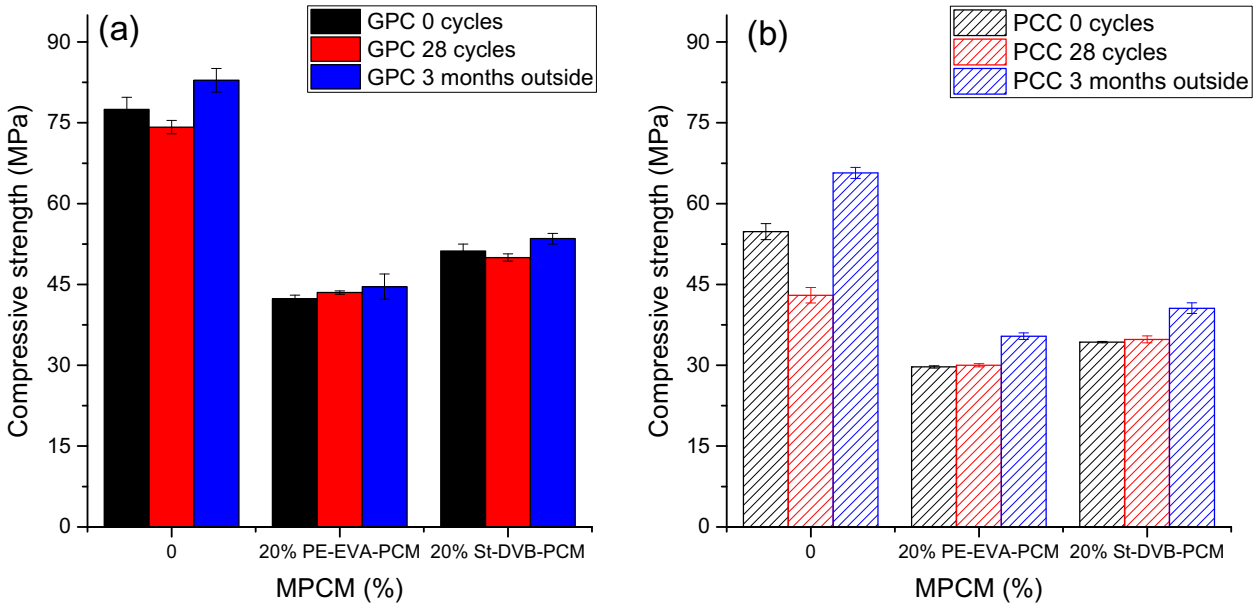

Fig. 9. The effect of MPCM on the compressive strength of 28 freeze-thaw cycles and of exposure to outdoor conditions for three months (a) GPC and (b) PCC.

by the presence of the other compounds. The 14 M NaOH solution is mixed with the sodium silicate solution with a solid content of 35%, and then with dry powders (which will adsorb water on the surface of the particles). When the resulting mixture (geopolymer paste) is cooled down to 0 °C at the start of the setting time measurements, it is reasonable to assume that both the NaOH and sodium silicate concentrations are higher than the solubilities of these components at 0 °C. Accordingly, the alkaline solution starts to precipitate. The solid particles formed from precipitation of the alkaline solution might act as nucleation sites for the geopolymerization process, thereby speeding up the reaction rate. In addition, the precipitation increases the solid content of the samples, which might contribute to shorter setting times.

4. Conclusion

The effect of freeze-thaw cycles on the physical and mechanical properties of GPC and PCC incorporated with two different types of MPCM was investigated. Microstructural studies illustrated that for both GPC and PCC microcracks appear in the interface between the paste and aggregates due to the expansion of capillary water during freeze-thaw cycles. These microcracks can contribute to the concrete deterioration. Crystals are formed in the PCC after exposure to freeze-thaw cycles.

The mass loss after 28 freeze-thaw cycles was less than 1% for all samples. The compressive strength of both GPC and PCC decrease after exposure to 28 freeze-thaw cycles. However, GPC

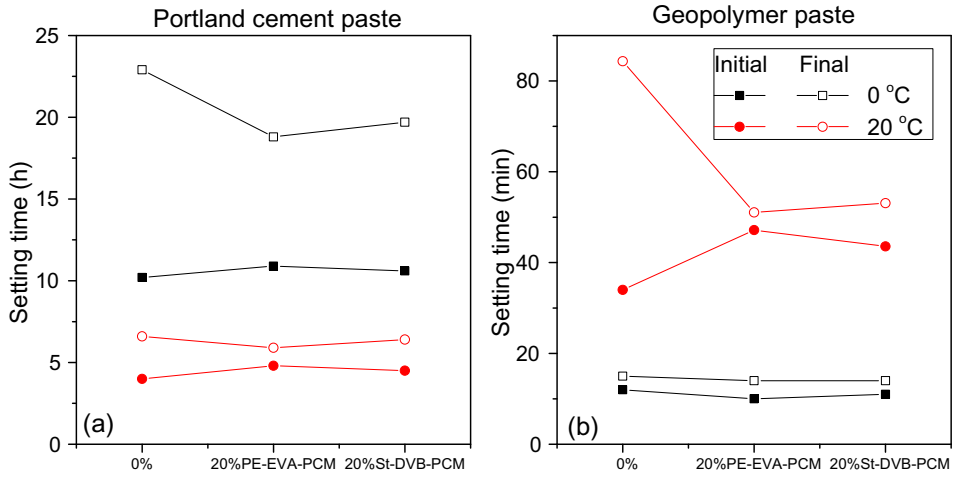

Fig. 10. The initial and final setting times of (a) Portland cement paste and (b) geopolymer paste containing 0 and 20 vol% of microcapsules at 0 °C and 20 °C.

exhibits a much better resistance against freeze-thaw cycles than PCC. Interestingly, after the addition of MPCM, the decrease in compressive strength after the freeze-thaw cycles was reduced to less than 2.5% after 28 days for all samples. This illustrates that the MPCM provides an excellent resistance against freeze-thaw cycles. Air voids and gaps between the microcapsules and the surrounding concrete provide free expansion space for water when it freezes, thereby reducing the frost induced stress.

The initial setting time became longer while the final setting time decreased with the addition of microcapsules. Water adsorbed onto the microcapsules is probably contributing to this effect. As expected, decreasing the temperature slowed down the reaction rate for Portland cement, causing longer setting times. Interestingly, the setting times for geopolymer pastes are much faster at low temperatures. This might be caused by precipitation of the alkaline solution at low temperatures.

Conflict of interest

The authors declare that we have no conflict of interest with respect to this paper.

Acknowledgement

We gratefully acknowledge funding from the Research Council of Norway, project number 238198. The authors acknowledge “Este trabajo es resultado de la actividad desarrollada en el marco del Programa de Ayudas a Grupos de Excelencia de la Región de Murcia, de la Fundación Séneca, Agencia de Ciencia y Tecnología de la Región de Murcia (Grant # 19877/GERM/15)”. We would like to thank Tonje Jensen for technical assistance.

Data availability

The raw/processed data required to reproduce these findings cannot be shared at this time as the data also forms part of an ongoing study.

References

[1] J. Davidovits, Geopolymer Chemistry and Applications, Institute Géopolymère, Saint-Quentin, France, 2011.
[2] M. Schneider, M. Romer, M. Tschudin, H. Bolio, Sustainable cement production—present and future, Cem. Concr. Res. 41 (7) (2011) 642–650.
[3] P. Duxson, J.L. Provis, G.C. Lukey, J.S.J. van Deventer, The role of inorganic polymer technology in the development of ‘green concrete’, Cem. Concr. Res. 37 (12) (2007) 1590–1597.
[4] W.K. Part, M. Ramli, C.B. Cheah, An overview on the influence of various factors on the properties of geopolymer concrete derived from industrial by-products, Constr. Build. Mater. 77 (2015) 370–395.
[5] B. Singh, G. Ishwarya, M. Gupta, S. Bhattacharyya, Geopolymer concrete: a review of some recent developments, Constr. Build. Mater. 85 (2015) 78–90.
[6] M.B. Karakoç, İ. Türkmen, M.M. Maraş, F. Kantarci, R. Demirboğa, M. Uğur Toprak, Mechanical properties and setting time of ferrochrome slag based geopolymer paste and mortar, Constr. Build. Mater. 72 (Supplement C) (2014) 283–292.
[7] S. Yaseri, G. Hajiaghaei, F. Mohammadi, M. Mahdikhani, R. Farokhzad, The role of synthesis parameters on the workability, setting and strength properties of binary binder based geopolymer paste, Constr. Build. Mater. 157 (Supplement C) (2017) 534–545.
[8] A. Karthik, K. Sudalaimani, C.T. Vijaya Kumar, Investigation on mechanical properties of fly ash-ground granulated blast furnace slag based self curing bio-geopolymer concrete, Constr. Build. Mater. 149 (Supplement C) (2017) 338–349.
[9] H. Marzouk, J. Kajiu, Effects of freezing and thawing on the tension properties of high-strength concrete, Mater. J., 91(6).
[10] J. Cao, D.D.L. Chung, Damage evolution during freeze–thaw cycling of cement mortar, studied by electrical resistivity measurement, Cem. Concr. Res. 32 (10) (2002) 1657–1661.
[11] D.P. Bentz, R. Turpin, Potential applications of phase change materials in concrete technology, Cem. Concr. Compos. 29 (7) (2007) 527–532.
[12] A.R. Sakulich, D.P. Bentz, Incorporation of phase change materials in cementitious systems via fine lightweight aggregate, Constr. Build. Mater. 35 (Supplement C) (2012) 483–490.
[13] A. Sharma, V.V. Tyagi, C.R. Chen, D. Buddhi, Review on thermal energy storage with phase change materials and applications, Renew. Sustain. Energy Rev. 13 (2) (2009) 318–345.
[14] T.-C. Ling, C.-S. Poon, Use of phase change materials for thermal energy storage in concrete: an overview, Constr. Build. Mater. 46 (2013) 55–62.
[15] A.F. Regin, S.C. Solanki, J.S. Saini, Heat transfer characteristics of thermal energy storage system using PCM capsules: a review, Renew. Sustain. Energy Rev. 12 (9) (2008) 2438–2458.
[16] D.-Q. Ng, Y.-L. Tseng, Y.-F. Shih, H.-Y. Lian, Y.-H. Yu, Synthesis of novel phase change material microcapsule and its application, Polymer 133 (Supplement C) (2017) 250–262.
[17] M. Song, F. Niu, N. Mao, Y. Hu, S. Deng, Review on building energy performance improvement using phase change materials, Energy Build. 158 (Supplement C) (2018) 776–793.
[18] V.D. Cao, S. Pilehvar, C. Salas-Bringas, A.M. Szczotok, J.F. Rodriguez, M. Carmona, N. Al-Manasir, A.-L. Kjøniksen, Microencapsulated phase change materials for enhancing the thermal performance of Portland cement concrete and geopolymer concrete for passive building applications, Energy Convers. Manage. 133 (2017) 56–66.
[19] N. Soares, J.J. Costa, A.R. Gaspar, P. Santos, Review of passive PCM latent heat thermal energy storage systems towards buildings’ energy efficiency, Energy Build. 59 (Supplement C) (2013) 82–103.
[20] A. Jayalath, R. San Nicolas, M. Sofi, R. Shanks, T. Ngo, L. Aye, P. Mendis, Properties of cementitious mortar and concrete containing micro-encapsulated phase change materials, Constr. Build. Mater. 120 (Supplement C) (2016) 408–417.
[21] M. Hunger, A.G. Entrop, I. Mandilaras, H.J.H. Brouwers, M. Founti, The behavior of self-compacting concrete containing micro-encapsulated Phase Change Materials, Cem. Concr. Compos. 31 (10) (2009) 731–743.
[22] S. Pilehvar, V.D. Cao, A.M. Szczotok, L. Valentini, D. Salvioni, M. Magistri, R. Pamies, A.-L. Kjøniksen, Mechanical properties and microscale changes of geopolymer concrete and Portland cement concrete containing micro-encapsulated phase change materials, Cem. Concr. Res. 100 (2017) 341–349.

[23] S. Jacobsen, E.J. Sellevold, Self healing of high strength concrete after deterioration by freeze/thaw, Cem. Concr. Res. 26 (1) (1996) 55–62.
[24] H. Yazıcı, The effect of silica fume and high-volume Class C fly ash on mechanical properties, chloride penetration and freeze–thaw resistance of self-compacting concrete, Constr. Build. Mater. 22 (4) (2008) 456–462.
[25] A. Allahverdi, M.M.B.R. Abadi, K.M. Anwar Hossain, M. Lachemi, Resistance of chemically-activated high phosphorous slag content cement against freeze–thaw cycles, Cold Regions Sci. Technol. 103 (Supplement C) (2014) 107–114.
[26] R. Slavik, V. Bednarik, M. Vondruska, A. Nemec, Preparation of geopolymer from fluidized bed combustion bottom ash, J. Mater. Process. Technol. 200 (1) (2008) 265–270.
[27] B.-W. Jo, S.-K. Park, J.-B. Park, Properties of concrete made with alkali-activated fly ash lightweight aggregate (AFLA), Cem. Concr. Compos. 29 (2) (2007) 128–135.
[28] A.M. Borreguero, J.L. Valverde, J.F. Rodríguez, A.H. Barber, J.J. Cubillo, M. Carmona, Synthesis and characterization of microcapsules containing Rubitherm®RT27 obtained by spray drying, Chem. Eng. J. 166 (1) (2011) 384–390.
[29] A.M. Szczotok, M. Carmona, A.-L. Kjøniksen, J.F. Rodriguez, Equilibrium adsorption of polyvinylpyrrolidone and its role on thermoregulating microcapsules synthesis process, Colloid Polym. Sci. 295 (5) (2017) 783–792.
[30] S. Pilehvar, V.D. Cao, A.M. Szczotok, M. Carmona, L. Valentini, M. Lanzón, R. Pamies, A.-L. Kjøniksen, Physical and mechanical properties of fly ash and slag geopolymer concrete containing different types of micro-encapsulated phase change materials, Constr. Build. Mater. 173 (2018) 28–39.
[31] M. Pania, X. Yunping, Effect of phase-change materials on properties of concrete, Mater. J., 109(1).
[32] L.A. Feldkamp, L.C. Davis, J.W. Kress, Practical cone-beam algorithm, J. Opt. Soc. Am. A 1 (6) (1984) 612–619.
[33] M. Lanzón, V. Cnudde, T. De Kock, J. Dewanckele, Microstructural examination and potential application of rendering mortars made of tire rubber and expanded polystyrene wastes, Constr. Build. Mater. 94 (2015) 817–825.
[34] M.A. González, E.F. Irassar, Ettringite formation in low C3A Portland cement exposed to sodium sulfate solution, Cem. Concr. Res. 27 (7) (1997) 1061–1072.
[35] I. Odler, J. Colán-Subauste, Investigations on cement expansion associated with ettringite formation, Cem. Concr. Res. 29 (5) (1999) 731–735.
[36] M.J. Setzer, Micro-ice-lens formation in porous solid, J. Colloid Interface Sci. 243 (1) (2001) 193–201.
[37] Z. Wang, Q. Zeng, L. Wang, K. Li, S. Xu, Y. Yao, Characterizing frost damages of concrete with flatbed scanner, Constr. Build. Mater. 102 (2016) 872–883.
[38] Y. Fu, L. Cai, W. Yonggen, Freeze–thaw cycle test and damage mechanics models of alkali-activated slag concrete, Constr. Build. Mater. 25 (7) (2011) 3144–3148.
[39] J.J. Valenza, G.W. Scherer, Mechanism for salt scaling, J. Am. Ceram. Soc. 89 (4) (2006) 1161–1179.
[40] L. Basheer, J. Kropp, D.J. Cleland, Assessment of the durability of concrete from its permeation properties: a review, Constr. Build. Mater. 15 (2) (2001) 93–103.
[41] M. Vancura, K. MacDonald, L. Khazanovich, Microscopic analysis of paste and aggregate distresses in pervious concrete in a wet, hard freeze climate, Cem. Concr. Compos. 33 (10) (2011) 1080–1085.
[42] P. Sun, H.-C. Wu, Chemical and freeze–thaw resistance of fly ash-based inorganic mortars, Fuel 111 (2013) 740–745.
[43] D. Niu, L. Jiang, Q. Fei, Deterioration mechanism of sulfate attack onnconcrete under freeze-thaw cycles, J. Wuhan Univ. Technol. Mater. Sci. Ed. 28 (6) (2013) 4.
[44] P.K. Dehdezi, M.R. Hall, A.R. Dawson, S.P. Casey, Thermal, mechanical and microstructural analysis of concrete containing microencapsulated phase change materials, Int. J. Pavement Eng. 14 (5) (2013) 449–462.
[45] H. Moosberg-Bustnes, B. Lagerblad, E. Forssberg, The function of fillers in concrete, Mater. Struct. 37 (2) (2004) 74.
[46] O. Coussy, P.J.M. Monteiro, Poroelastic model for concrete exposed to freezing temperatures, Cem. Concr. Res. 38 (1) (2008) 40–48.
[47] A. Allahverdi, S. Pilehvar, M. Mahinroosta, Influence of curing conditions on the mechanical and physical properties of chemically-activated phosphorous slag cement, Powder Technol. 288 (2016) 132–139.
[48] M.M. Kamal, M.A. Safan, A.A. Bashandy, A.M. Khalil, Experimental investigation on the behavior of normal strength and high strength self-curing self-compacting concrete, J. Build. Eng. 16 (2018) 79–93.
[49] S. Ismail, W.H. Kwan, M. Ramli, Mechanical strength and durability properties of concrete containing treated recycled concrete aggregates under different curing conditions, Constr. Build. Mater. 155 (2017) 296–306.
[50] J.I. Escalante-García, J.H. Sharp, Effect of temperature on the hydration of the main clinker phases in Portland cements: part i, neat cements, Cem. Concr. Res. 28 (9) (1998) 1245–1257.
[51] V.D. Cao, S. Pilehvar, C. Salas-Bringas, A.M. Szczotok, L. Valentini, M. Carmona, J.F. Rodriguez, A.-L. Kjøniksen, Influence of microcapsule size and shell polarity on thermal and mechanical properties of thermoregulating geopolymer concrete for passive building applications, Energy Convers. Manage. 164 (2018) 198–209.
[52] D.P. Bentz, A review of early-age properties of cement-based materials, Cem. Concr. Res. 38 (2) (2008) 196–204.
[53] D.P. Bentz, Cement hydration: building bridges and dams at the microstructure level, Mater. Struct. 40 (4) (2007) 397–404.
[54] L. Wadsö, F. Winnefeld, K. Riding, P. Sandberg, Calorimetry, in: K. Scrivener, R. Snellings, B. Lothenbach (Eds.), A practical guide to microstructural analysis of cementitious materials, Taylor & Francis, 2016, pp. 37–74.
[55] U. Rattanasak, P. Chindaprasirt, Influence of NaOH solution on the synthesis of fly ash geopolymer, Miner. Eng. 22 (12) (2009) 1073–1078.
[56] P. Sashi, A.K. Bhuyan, Viscosity dependence of some protein and enzyme reaction rates: seventy-five years after Kramers, Biochemistry 54 (29) (2015) 4453–4461.
[57] A. Kumar, S.S. Pawar, High viscosity of ionic liquids causes rate retardation of Diels-Alder reactions, Sci. China-Chem. 55 (8) (2012) 1633–1637.